



Integrated Frame Coding for Short Burst Transmission in Mobile Visible Light Communication Systems

Jing-Shu Xue , Yan-Yu Zhang, and Yi-Jun Zhu 

Abstract—Recently, visible light communication (VLC) has become a promising option for secure data transmission in industrial Internet of Things (IIoTs). In IIoT-VLC systems, small attocells are adopted to achieve higher spatial reuse rate, and the transmission of data, control and feedback bursts often requires high efficiency and real-time feature. Conventionally, multi-field (MF) frames are used in VLC systems which consists of sync header, channel training sequence, check field, etc. in addition to data payload. However, for short burst transmission, MF frames could result in efficiency loss and latency increase due to useless padding bits. In this paper, a novel coding scheme named integrated frame code (IFC) in physical layer to realize efficient and real-time transmission simultaneously is presented. IFC scheme reduces latency by simplifying transmission procedure and decreases overhead redundancy by integrated design. Specifically, we propose a joint soft-decision criterion for receiving without separate synchronization and channel estimation and then analyze its error performance. After that, we present IFC construction criterion and two design examples. At last, simulation results confirm that for short burst transmission, IFC achieves better efficiency and robustness than MF especially in moving process.

Index Terms—Attocell, frame coding, industrial internet of things, visible light communication.

I. INTRODUCTION

RECENTLY, visible light communication (VLC) with inherent security feature has become a promising option to realize secure data transmission in industrial Internet of Things (IIoTs) [1]–[4]. In IIoT-VLC systems, small attocells are densely distributed to achieve higher spatial reuse rate, and diverse mobile users require varies of data for status monitoring, action control and reaction feedback, most of which are short bursts and thus desiring higher efficiency and lower latency transmission [5]–[9].

Traditionally, data to be transmitted are organized into several multi-field (MF) long frames in data link layer, which mainly include overheads of sync header, channel training field and

check field in addition to data payload [10]. However, for short burst transmission, a large amount of useless padding bits should be added in order to keep long frame length, leading to a decrease in communication efficiency [11]. Meanwhile, receiving a lot of useless data could also cause latency increase. Additionally, channel factors estimated by channel training sequences at head of each frame could has larger error for rear bits in the process of receivers' movement over attocells, and thus resulting in receiving deterioration [12]. Therefore, long MF frames are no longer suitable for short burst transmission in IIoT-VLC systems.

Nevertheless, if we merely shorten the MF frame, the proportion of fixed length overhead for channel training, synchronization and anti-noise coding will be greatly increased, which could also cause efficiency loss. Also, the fields being serially generated and processed could extend time latency at both transmitting and receiving end. Consequently, neither long nor short MF frame could achieve high efficiency and low latency transmission of short bursts, which has brought a great challenge to IIoT-VLC system.

Inspired by [13] which integrates frame acquisition, carrier recovery and carrier phase tracking into pilot symbols, we want to propose a novel coding scheme named integrated frame code (IFC) in physical layer to realize efficient and real-time transmission for short burst data in IIoT-VLC systems. IFC replaces the channel training sequence of MF frame by averaging the receiving signal power for channel estimation, and removes the sync header and check field by introducing the squared shifting Euclidean distance (SSED) in code construction and signal decision for simultaneous synchronization and error correction. Therefore, the integrated design compresses the overhead length in short frames, thereby increasing communication efficiency. Meanwhile, different from MF frame which requires multi-step generation and processing, short frames generated in one step using IFC could realize robust transmission without serial processes of different fields, which greatly simplifies transmission procedure and may improve the real-time feature.

To sum up, our contributions could be summarized as follows.

- 1) We establish a complete VLC coding scheme with IFC. At transmitters, burst data is coded to short IFC frames and then transmitted by Lambert sources. At receivers, soft-decision are jointly operated without separate synchronization and channel estimation, and then signals are decoded to transmitted messages.

Manuscript received October 6, 2021; revised December 29, 2021; accepted January 16, 2022. Date of publication January 21, 2022; date of current version February 2, 2022. The work was supported in part by the National Key Research and Development Project under Grant 2018YFB1801903, in part by the National Natural Science Foundation of China under Grants 61671477 and 61901524, and in part by the China Postdoctoral Science Foundation under Grant 2019M663477. (Corresponding author: Yi-Jun Zhu.)

The authors are with the Information Engineering University, Zhengzhou, Henan Province 450000, China (e-mail: xjslovesstudy@163.com; xindazhang@126.com; yijunzhu@zzu.edu.cn).

Digital Object Identifier 10.1109/JPHOT.2022.3144408

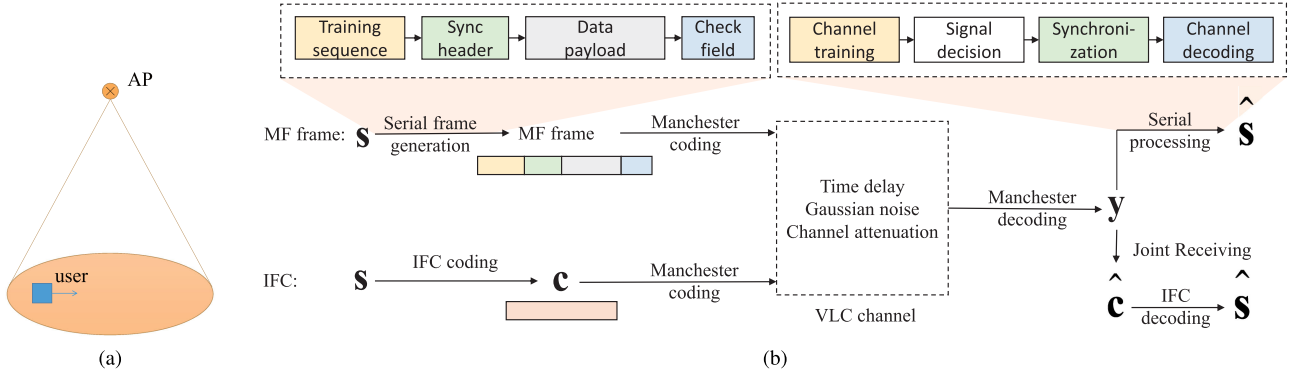


Fig. 1. Diagram of (a) mobile VLC in an attocell and (b) transmission process with MF frame or IFC.

- 2) We figure out the joint soft-decision criterion which integrates synchronization and anti-noise receiving, and the error performance of this criterion is analyzed. After that, we specify the code set construction objective for IFC with SSED as the core, and two design examples of binary code are given.
- 3) We verify the synchronization and the anti-noise abilities of IFC scheme under different frame lengths and channel conditions by simulation. The results also demonstrate that IFC achieves higher efficiency and better robustness to noise and movement in mobile VLC systems.

The remainder of this paper is organized as follows. In Section II, we introduce the transmitting and receiving system with IFC. After that, the joint soft-decision method is detailedly proposed and analyzed in Section III. Then, in Section IV, we present the construction criterion and two IFC examples. Afterwards, the previous theorems are verified and the performance of IFC system is explored by simulation in Section V. Finally, our paper is concluded in Section VI.

II. SYSTEM MODEL

In this paper, we consider a single-input single-output mobile VLC system with IFC as Fig. 1(a), where users move in the coverage of one AP. In Fig. 1(b), the transmission processes of system with MF frame and IFC are presented. Unlike in system with MF frame which has serial processes of frame generation and signal recovery, IFC system has coding and decoding processes which can be operated in one step. Meanwhile, the IFC frame is shorter than the MF frame by integrating design. Both properties improve the efficiency and decrease the latency [14]. Note that we do not consider inter-attocell interference in this paper [15], [16]. Next, let us introduce the three key links of short burst transmission with IFC.

At transmitters, message \mathbf{s} of a constant length is coded to an M -ary IFC $\mathbf{c} = [c_0 c_1 \cdots c_{N-1}]^T$ without serial adding of sync header, channel training sequence and check field like in MF frame. Here, the length of \mathbf{c} is N , and $\mathbf{c} \in \mathcal{C} = \{\gamma_1, \gamma_2, \dots, \gamma_K\}$. The code set \mathcal{C} is composed of K non-zero code elements. Note that every code element γ_k is transmitted with equal probability, i.e. $P(\mathbf{c} = \gamma_k) = \frac{1}{K}$ for $k = 1, 2, \dots, K$, and when no message is transmitted, $\mathbf{c} = \mathbf{0}$.

On the basis of IFC coding, we also operate Manchester coding and decoding respectively at transmitters and receivers in order to ensure the continuity of lighting and the relative constancy of average power [17]. Because Manchester coding could be realized by detecting rising and falling edges of received signals without additional symbol synchronization, and the coding and decoding processes do not change the probability distribution of additive Gaussian noise, we ignore the influence of both Manchester coding and decoding in our research.

In VLC channel, both transmitted signals simultaneously suffer time delay, Gaussian noise and channel attenuation. In MF frame, synchronization is carried out before data recovery, and thus the random transmission delay can be ignored in subsequent operations. However, in IFC, the position of the first bit of every short frame in received signals is unknown because of the lack of sync header and synchronization in advance. Therefore, we first discuss the time delay without considering channel attenuation and Gaussian noise. We suppose that the sampling starts early enough and persists long enough so that \mathbf{c} could be completely received. Hence, the received signal without channel influence could be equivalent to

$$\mathbf{x}^{(\mathbf{c}, m_0)} = [\mathbf{0}_{1 \times m_0} \mathbf{c}^T \mathbf{0}_{1 \times (L-N-m_0)}]_{1 \times L}^T \quad (1)$$

where L is sampling length and m_0 is named sampling delay. In addition, m_0 follows a discrete uniform distribution from 0 to $L - N$.

On the basis of the delayed signal, we also adopt a mostly used VLC channel model as (2) [18]

$$\mathbf{y} = h\mathbf{x}^{(\mathbf{c}, m_0)} + \mathbf{v} \quad (2)$$

Among them, $\mathbf{v} = [v_0 v_1 \cdots v_{L-1}]^T$ is an additive Gaussian noise satisfying $v_i \sim N(0, \sigma^2)$ for $i = 0, 1, \dots, L - 1$. Meanwhile, h is the channel factor between Lambertian source and the receiver that follows [19], [20]

$$h = \frac{(\alpha + 1) A_R \delta}{2\pi d^2} \cos^\alpha \phi \cos \psi \quad (3)$$

where ϕ is the radiation angle of light source and ψ is the incident angle of light at receivers. Also, m is the lighting order of Lambertian sources following $\alpha = -\ln 2 / \ln(\cos \psi_{0.5})$, and $\psi_{0.5}$ is the semi-power angle of light sources. Additionally, A_R is the area of detecting sensors, δ is the detecting responsivity [21],

and d is the distance between light and receiver. In addition, for the bursts transmitted at a high data rate, the duration of one frame is very short compared with the time that users take to go across an attocell. Therefore, we assume that h is constant in a frame period.

At receivers, unlike the serial signal processing of MF frame, in IFC, the channel is estimated by averaging the receiving signal power and the transmitted frame $\hat{\mathbf{c}}$ is determined based on sampled signals \mathbf{y} with noise interference and unknown m_0 . After that, the determined signals are decoded to $\hat{\mathbf{s}}$ by mapping methodology. In this paper, our main task is to properly design an efficient IFC code set \mathcal{C} which is robust to noise interference and random time delay and to propose a joint synchronization, channel estimation and anti-noise signal soft-decision cooperated with IFC scheme.

III. JOINT SOFT-DECISION FOR IFC

In this section, we establish the joint synchronization, channel estimation and anti-noise soft-decision criterion of IFC system. Meanwhile, its the error performance is also analyzed.

Here, we apply the maximum-likelihood (ML) criterion to jointly decide the transmitted frame \mathbf{c} and sampling delay m_0 from \mathbf{y} [22], [23]. First, the transition probability density function is given by

$$f(\mathbf{y} | \gamma_k, m) = \frac{1}{(\sqrt{2\pi}\sigma)^L} e^{-\frac{\|\mathbf{y}\|^2 + h^2 \|\gamma_k\|^2 - 2hR_{\gamma_k \mathbf{y}}(m)}{2\sigma^2}}, \forall k, m \quad (4)$$

where m is any probable sampling delay, γ_k is any code element, $\|\mathbf{y}\|^2$ and $\|\gamma_k\|^2$ represent the squared 2-norm of \mathbf{y} and γ_k , and $R_{\gamma_k \mathbf{y}}(m) = \sum_{i=0}^{N-1} \gamma_{k,i} y_{i+m}$. When σ is constant, we could get ML soft-decision criterion of IFC

$$\begin{aligned} (\hat{\mathbf{c}}, \hat{m}) &= \arg \max_{\gamma_k, m} l(\gamma_k, m) \\ &= \arg \max_{\gamma_k, m} \left[2R_{\gamma_k \mathbf{y}}(m) - \hat{h} \|\gamma_k\|^2 \right] \end{aligned} \quad (5)$$

where $\hat{\mathbf{c}}$, \hat{m} and \hat{h} are the estimated value of \mathbf{c} , m_0 and h . Here, \hat{h} is estimated by averaging received Manchester coded signals. Then, Property 1 is satisfied in terms of the performance of the proposed joint soft-decision criterion. Its proof is shown in Appendix A.

Property 1: The error decision probability of the joint soft-decision criterion is upper bounded by

$$P((\hat{\mathbf{c}}, \hat{m}) \neq (\mathbf{c}, m_0)) \leq \frac{\sum_{m_i} \sum_{m_j} \sum_{\gamma_i} \sum_{\gamma_j} Q\left(\frac{h}{2\sigma} \sqrt{D^2(\gamma_i, \gamma_j, \Delta m)}\right)}{K(L - N + 1)} \quad (6)$$

where $\gamma_i, \gamma_j \in \mathcal{C}$, and

$$D^2(\gamma_i, \gamma_j, \Delta m) = \begin{cases} \|\mathbf{x}^{(\gamma_i, 0)} - \mathbf{x}^{(\gamma_i, \Delta m)}\|^2, & \Delta m \geq 0 \\ \|\mathbf{x}^{(\gamma_i, 0)} - \mathbf{x}^{(\gamma_j, -\Delta m)}\|^2, & \Delta m < 0 \end{cases} \quad (7)$$

where $\Delta m = m_i - m_j$. ■

In (7), $D^2(\gamma_i, \gamma_j, \Delta m)$ degrades into the squared Euclidean distance $\|\gamma_i - \gamma_j\|^2$ when $\Delta m = 0$. Meanwhile, when $\Delta m \neq 0$, $D^2(\gamma_i, \gamma_j, \Delta m)$ could be regarded as the squared Euclidean

distance (SED) between the shifted γ_i and γ_j , and thus being defined as SSED, which is very essential to IFC construction [24].

IV. IFC CONSTRUCTION

In this section, we first set the construction criterion of IFC code set. According to the criterion, two design examples are analytically presented.

A. Design Criterion

According to (6), error decision rate is determined by SSED when h and σ is constant in a frame period. Thus, we give the design criterion of IFC construction as

$$\begin{aligned} \arg \max_{\mathcal{C}} \min_{i,j,\Delta m} D^2(\gamma_i, \gamma_j, \Delta m) \\ \gamma_i^{(0)} \neq \gamma_j^{(\Delta m)} \quad \textcircled{1} \\ s.t. \Delta m \geq 0 \quad \textcircled{2} \end{aligned} \quad (8)$$

In order to promote the coding robustness to noise and uncertain sampling delay, our optimization objective is to maximize the minimum value of SSED under the constraints. Specifically, $\textcircled{1}$ is used to prevent fuzzy decision, i.e. the case that SSED = 0. $\textcircled{2}$ is used to avoid repeated search caused by code sets' symmetrical feature. If we adjust the parameters M , N and K , code sets for different efficiency and robustness requirements could be constructed.

B. Design Examples

On the basis of the proposed design objective, we could construct IFC by exhausting searching. However, for some relatively simple cases, IFC could be analytically constructed. Next, two binary examples will be presented.

In order to simplify the code design, we utilize an equivalence property between different code sets. Before we introduce the property, the definition of equivalent shifting is given.

Definition 1: The transition from sequence $\gamma_k = [\mathbf{0}_{1 \times \tilde{m}_0} \alpha_{1 \times n}^T \mathbf{0}_{1 \times (N-n-\tilde{m}_0)}]_{1 \times N}^T \in \mathcal{C}$ to $[\mathbf{0}_{1 \times \tilde{m}} \alpha_{1 \times n}^T \mathbf{0}_{1 \times (N-n-\tilde{m})}]_{1 \times N}^T$ is named as equivalent shifting, where the first and the last elements of α are nonzero and $\tilde{m}_0, \tilde{m} = 0, 1, 2, \dots, N - n$.

It is not difficult to obtain that equivalent shifting on elements of $\mathcal{C} = \{\gamma_1, \gamma_2, \dots, \gamma_K\}$ does not change the minimum SSED of the code set \mathcal{C} . Therefore, code set \mathcal{C} is equivalent to $\mathcal{C}_{\mu_1} = \{\gamma_k | \gamma_k = [\mathbf{0}_{1 \times (N-n_k)} \alpha_{1 \times n_k}^{(k)T}]_{1 \times N}^T\}$ for binary code i.e. $M = 2$, which could be rewritten as $\mathcal{C}_{\mu_1} = \{\gamma_k | \gamma_k = [\mu_{1 \times (N-1)}^{(k)T} \mathbf{1}]_{1 \times N}^T\}$ because the last element of α is '1'. Then, *Property 2* is workable, the proof of which is shown in Appendix B.

Property 2: If $\gamma^{(i)}, \gamma^{(j)} \in \mathcal{C}_{\mu_1}$, then SSED between $\gamma^{(i)}$ and $\gamma^{(j)}$ is increased by two or stays the same under different cases compared with $\{\gamma_k | \gamma_k = \mu_{1 \times (N-1)}^{(k)}\}$. ■

According to *Property 2*, the addition of '1' on the code set $\{\gamma_k | \gamma_k = \mu_{1 \times (N-1)}^{(k)}\}$ could ensure that $\min \text{SSED} \neq 0$, which is equivalent to the first constraint in (8). Thus, we obtain Theorem 1 and Theorem 2 to construct code sets with $\min \text{SSED} = 1$ or 2.

Theorem 1: If $\mu^{(k)}$ in $\mathcal{C}_{\mu 1}$ traverse all the binary sequences from 0 to $2^N - 1$ as follows, then $\min \text{SSED} = 1$.

$$\begin{aligned} \gamma_1 &: 000 \cdots 001 \\ \gamma_2 &: 000 \cdots 011 \\ \gamma_3 &: 000 \cdots 101 \\ &\vdots \\ \gamma_{2^{N-1}} &: 111 \cdots 101 \\ \gamma_{2^N} &: 111 \cdots 111 \end{aligned}$$

Proof: When $\Delta m = 0$, it is not difficult to get that $\text{SSED} \neq 0$. For $\Delta m \neq 0$, $b = 1$ corresponds to the last '0' of the shifted γ_i , and thus $\text{SSED} \geq 1$. ■

Theorem 2: We arrange $\{\mu^{(k)}\}$ of Theorem 1 in Gray code order, and then add '1' after each code [25]. After that, we divide them into two sets according to odd and even of the ordinal numbers as follows

$$\begin{aligned} \gamma_1^{(1)} &: 000 \cdots 001 \\ \gamma_1^{(2)} &: 000 \cdots 011 \\ \gamma_2^{(1)} &: 000 \cdots 111 \\ \gamma_2^{(2)} &: 000 \cdots 101 \\ &\vdots \\ \gamma_{2^{N-1}}^{(1)} &: 100 \cdots 011 \\ \gamma_{2^{N-1}}^{(2)} &: 100 \cdots 001 \end{aligned}$$

then both code sets $\mathcal{C}_1 = \{\gamma_1^{(1)}, \gamma_2^{(1)}, \dots, \gamma_{2^{N-1}}^{(1)}\}$ and $\mathcal{C}_2 = \{\gamma_1^{(2)}, \gamma_2^{(2)}, \dots, \gamma_{2^{N-1}}^{(2)}\}$ satisfy $\min \text{SSED} = 2$. ■

The proof of Theorem 2 is in Appendix C. We adopt \mathcal{C}_2 which is with larger minimum code weight to distinguish from non-signal case, namely the all-zero sequence.

Our theorems only cost 1 b overhead make $\min \text{SSED} = 1$ and 2 bits to make $\min \text{SSED} = 2$ for frames of all lengths. Therefore, we believe that IFC scheme is efficient especially for short burst transmission.

V. SIMULATION

In this section, we verify the correctness of previous findings about joint decision performance and IFC construction criterion. Meanwhile, the synchronization and anti-noise receiving abilities are tested by simulation. Moreover, comparison of IFC and MF scheme in mobile system is also carried out. Note that in our simulation, message sequences are randomly mapped to code elements, indicating that IFC could probably achieve better performance than our results if mapping algorithm is elaborately designed.

A. Verification of Property 1 and IFC Design Criterion

In previous sections, we have derived the upper bound of error decision rate i.e. *Property 1*, and based on which IFC construction criterion has been proposed. In order to verify them, we compute the analytical upper bound and simulate the error decision rate of code sets in Table I under different

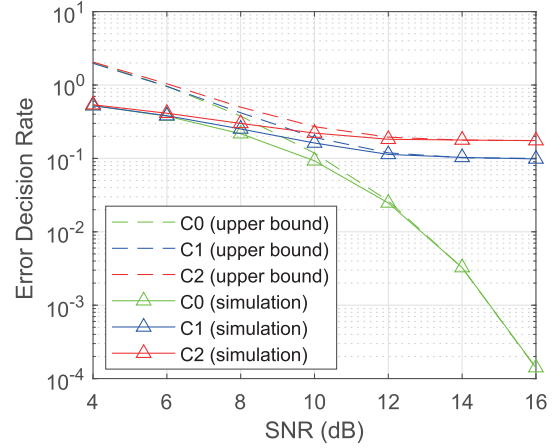


Fig. 2. Error determination rate of code sets with different min SSEDs.

signal-to-noise ratios (SNRs), which is shown in Fig. 2. As we can see, the results by simulation approach upper bound when $\text{SNR} \geq 12\text{dB}$, implying that the analyzed upper bound could represent error decision rate under high SNR. Meanwhile, for both analyzed and simulated results, code sets with larger min SSED perform better under the same SNR, and error floor occurs when $\min \text{SSED} = 0$, which reflects the rationality of our IFC construction criterion.

B. Synchronization and Anti-Noise Performance

In this part, we first explore the anti-noise performance of IFC constructed by Theorem 2 under perfect synchronization. Hence, SSED degrades into SED and thus the last '1' of each code could be removed. In Fig. 3, we present the frame error rate (FER) and bit error rate (BER) of on-off keying transmission with or without IFC. The results illustrate that IFC with only 1 b coding overhead achieves an obvious error rate reduction especially under high SNR. Moreover, the BER performance enhancement of short frames with different lengths is relatively close to each other, which we believe could improve applicability of our scheme.

Next, we consider both synchronization and noise resistance performance of our scheme. In this simulation, we compare IFC scheme with MF frame transmission, which adopts a relatively simple frame structure with a PN sync header of length L_s before binary message sequence of length L_m [26]. Considering the short frame length, check field is not added after data payload, and receivers use sliding correlation for signal synchronization [27]. In IFC scheme, integrated frame code constructed by Theorem 2 and joint soft-decision method are utilized at receivers. In Fig. 4, when $\text{SNR} < 10\text{dB}$ and $L_s = 15$, the scheme with MF frame outperforms the proposed scheme on both BER and synchronization. This is because IFC with only 2 bits overhead for both synchronization and error decrease cannot resist the huge noise, and thus leading to error synchronization and recovery (especially the error synchronization which severely increases BER), while the sliding correlation synchronization with long sync header is more robust to the noise, which however costs more overheads and efficiency. For

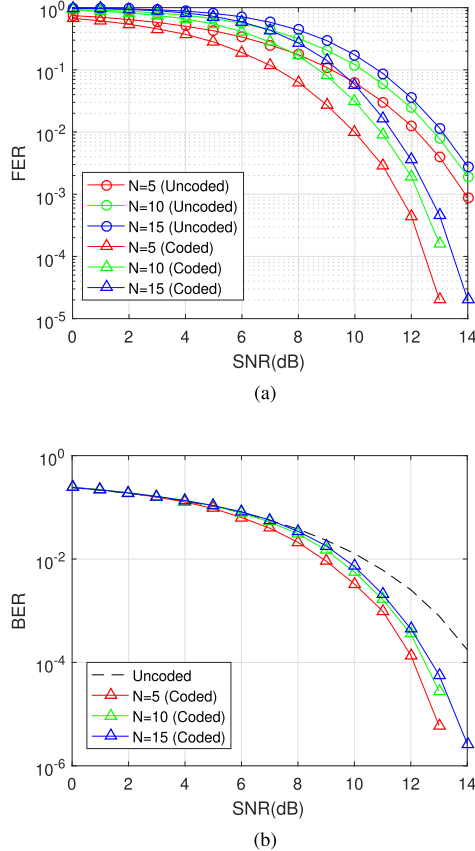
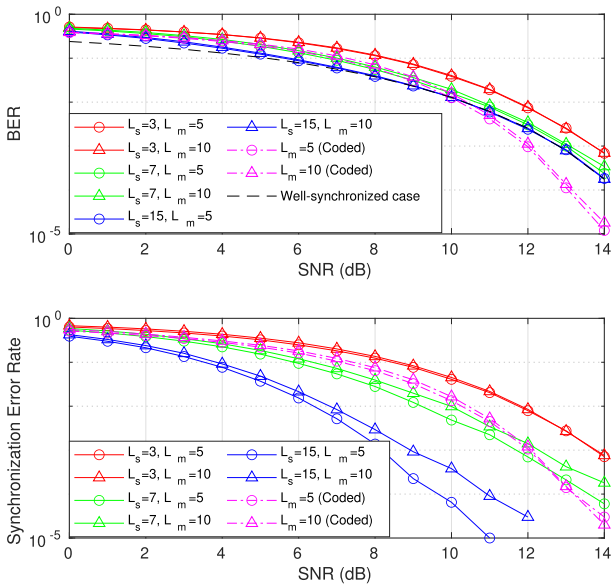

 Fig. 3. (a) FER and (b) BER under different N and SNR with or without IFC.


Fig. 4. BER and Synchronization error rate under different SNR.

the case when $\text{SNR} \geq 10\text{dB}$, IFC system presents smaller BER than the upper bound of MF method (i.e. the BER when synchronization is perfectly operated) because of the anti-noise coding and soft-decision. In terms of synchronization performance, IFC scheme with 2 bits cost has an approximate error rate to the

 TABLE I
 SETUP OF ERROR DECISION SIMULATION

i	\mathcal{C}_i	min SSED
1	{1111,1110,1101,1011,1001,1010,0100,1000}	0
2	{1111,1110,1101,1011,1001,1010,1100,1000}	1
3	{0001,0111,1101,1011}	2

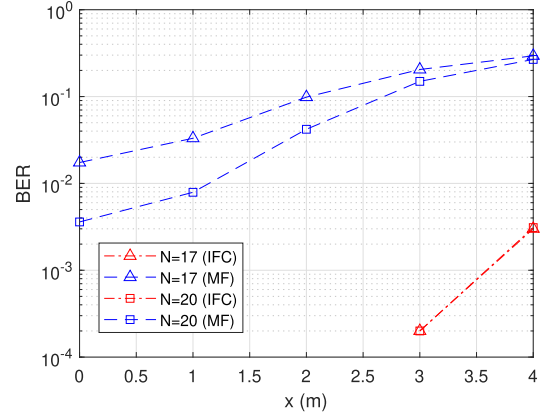


Fig. 5. BER of different receiver locations under different transmission schemes.

$L_s = 7$ case under the given message length, indicating that IFC could achieve great synchronization and receiving for short frame and under proper channel condition.

C. Simulation in Mobile VLC System

Now, we explore the receiving performance of IFC and MF scheme in a mobile VLC system which is set up as Table II. We consider two groups of comparison for IFC and MF. In each group, frame length N and message length L_m are the same. Here, we use IFC constructed by Theorem 2 in IFC scheme. However, in MF schemes, sync headers are added, and sliding correlation is used for synchronization. Meanwhile, we adopt 8-ary modulation to ensure the same short frame length with IFC scheme, and thus RS codes of different formats are also utilized for robustness improvement. In Fig. 5, we present the BER distribution of different receiver locations. Here, x is the distance between the receiver and the vertical projection of the light source on floor. As we can see, the BER of both schemes deteriorates with the increase of users' distance from AP because of the increasing channel attenuation and the decreasing SNR. Nevertheless, for the simulated locations, BER of IFC demonstrates a great superior compared with MF scheme and always keeps at a very low level, which indicates an increase of APs' communication coverage and the save of power consumption. Additionally, because of the frame length limitation, we do not add a channel training sequence and assume that receivers know the channel factors of every position in MF scheme, which is idealized and would make the result of MF higher than actual value. Consequently, the simulation demonstrates that the integrated scheme performs better for short burst transmission in mobile VLC system.

TABLE II
SYSTEM SIMULATION SETUP

Category	Parameter	Symbol	Value
System	Transmitting power	P_r	150W
	Semi-angle of half power	ϕ	45°
	Symbol rate	R_s	5Mbps
	Diameter of photon detector (PD)	d	3.0mm
	PD's detecting reponsivity	δ	0.5A/W
	Equivalent noise power	-	$3.5 \times 10^{-19} \text{W/Hz}^{0.5}$
	Receiver's PD number	-	64
$N=17, L_m=15$	IFC	Modulation	-
		Modulation	-
	MF	Sync header length	L_s
		Channel coding	-
$N=20, L_m=18$	IFC	Modulation	-
		Modulation	-
	MF	Sync header length	L_s
		Channel coding	-

VI. CONCLUSION

In this paper, we have proposed an IFC method for short burst transmission in mobile IIoT-VLC system. We introduced the transmitting and receiving VLC model with IFC. Under the system, we proposed a joint soft-decision algorithm which realizes anti-noise receiving without separate synchronization and also explored its performance upper bound. According to the upper bound, a design criterion of IFC was raised, and two design examples were analytically presented. Finally, our simulations have verified the upper bound and design criterion. The results have also demonstrated that IFC could achieve efficient and robust transmission especially for short burst data under high SNR. At last, the enhancement of IFC scheme compared with MF scheme in mobile VLC system has also been verified.

APPENDIX A

THE PROOF OF PROPERTY 1

(9) is the error probability when actual values are γ_k and m_0 while the estimated values are γ_β and m .

$$\begin{aligned}
 & P \{l(m_0, \gamma_k) < l(m, \gamma_\beta) | \gamma_k, m_0\} \\
 &= P \left\{ R_{\gamma_k \mathbf{y}}(m_0) - R_{\gamma_\beta \mathbf{y}}(m) < \hat{h} \frac{\|\gamma_k\|^2 - \|\gamma_\beta\|^2}{2} \middle| \gamma_k, m_0 \right\} \\
 &= P \left\{ V(\gamma_k, \gamma_\beta, \Delta m) < \hat{h} \left(R_{\gamma_\beta \gamma_k}(\Delta m) - \frac{\|\gamma_k\|^2 + \|\gamma_\beta\|^2}{2} \right) \right\} \quad (9)
 \end{aligned}$$

Here, $V(\gamma_k, \gamma_\beta, \Delta m) = \sum_{i=0}^{N-1} \gamma_{k,i} v_{i+m_0} - \sum_{i=0}^{N-1} \gamma_{\beta,i} v_{i+m}$. According to the independence of v_i , the left part of (9) satisfies $V(\gamma_k, \gamma_\beta, \Delta m) \sim N(0, D(\gamma_k, \gamma_\beta, \Delta m)\sigma^2)$. Meanwhile, $D^2(\gamma_k, \gamma_\beta, \Delta m) = \|\gamma_k\|^2 + \|\gamma_\beta\|^2 - 2R_{\gamma_\beta \gamma_k}(\Delta m)$. Then, (9) can be simplified to $Q(\frac{\hat{h}}{2\sigma} D(\gamma_k, \gamma_\beta, \Delta m))$. If signal sample is long enough to make $\hat{h} \approx h$, then the conditional error probability presetting a certain transmitted sequence and sampling delay could be upper bounded by

$$P((\hat{s}, \hat{m}) \neq (s, m_s) | \gamma_k, m_0)$$

$$\begin{aligned}
 & \leq \sum_{\gamma_\beta} \sum_{\Delta m} P \{l(m_0, \gamma_k) < l(m, \gamma_\beta) | \gamma_k, m_0\} \\
 &= \sum_{\gamma_\beta} \sum_{\Delta m} Q \left(\frac{h}{2\sigma} D(\gamma_k, \gamma_\beta, \Delta m) \right)
 \end{aligned}$$

Finally, using the total probability formula, it is not difficult to get *Property 1*. ■

APPENDIX B

THE PROOF OF PROPERTY 2

We denote $\mathcal{C}_{\mu 0} = \{\gamma_k | \gamma_k = [\mu_{1 \times (N-1)}^{(k)T} 0]_{1 \times N}^T\}$, which evidently has the same SSED with the code set $\{\gamma_k | \gamma_k = \mu_{1 \times (N-1)}^{(k)}\}$. We explore the impact of '1' at the end of each code in $\mathcal{C}_{\mu 1}$ by comparing SSED between codes of $\mathcal{C}_{\mu 1}$ and $\mathcal{C}_{\mu 0}$.

Case 1: When $\Delta m = 0$, $D^2(\gamma_i, \gamma_j, 0) = \|\mu^{(i)} - \mu^{(j)}\|^2$ for both $\mathcal{C}_{\mu 1}$ and $\mathcal{C}_{\mu 0}$.

Case 2: When $\Delta m \neq 0$, we present the shifted $\gamma_i, \gamma_j \in \mathcal{C}_{\mu 0}$ or $\mathcal{C}_{\mu 1}$ as

$$\begin{aligned}
 i: & \mu_0^{(i)} \cdots \mu_{\Delta m}^{(i)} \cdots a & 0 & \cdots 0 \\
 j: & 0 \cdots \mu_0^{(j)} \cdots \mu_{N-1-\Delta m}^{(j)} & \mu_{N-\Delta m}^{(j)} & \cdots b
 \end{aligned}$$

where $a = b = 0$ for $\mathcal{C}_{\mu 0}$, and $a = b = 1$ for $\mathcal{C}_{\mu 1}$. For $\mathcal{C}_{\mu 0}$, if we convert b from '0' to '1,' SED between γ_i and γ_j will be increased by one. Meanwhile, when converting a from '0' to '1,' SSED will be increased by one if $\mu_{N-1-\Delta m}^{(j)} = 0$, and if $\mu_{N-1-\Delta m}^{(j)} = 1$, SSED will be decreased by one. In summary, *Property 2* is workable. ■

APPENDIX C

THE PROOF OF THEOREM 2

As we know, the Gray codes $\{\mu^{(k)}\}$ of \mathcal{C}_1 have a mapping relationship with natural binary codes. Meanwhile, it is not difficult to obtain that the lowest bit of every corresponding natural binary code is '0'. Therefore, the following mapping relationship is workable.

$$\begin{aligned}
 \text{Bin: } & b_0 \ b_1 \ \cdots \ b_n \ \cdots \ b_{N-3} \ \ 0 \\
 \mu^{(k)}: & b_0 \ b_0 \oplus b_1 \ \cdots \ b_{n-1} \oplus b_n \ \cdots \ b_{N-2} \oplus b_{N-3} \ b_{N-3}
 \end{aligned}$$

where \oplus means modulo 2 addition.

For the case $\Delta m = 0$, we assume that $\exists \gamma_i^{(1)}, \gamma_j^{(1)} \in \mathcal{C}_1, i \neq j$, which satisfy $D^2(\gamma_i^{(1)}, \gamma_j^{(1)}, 0) = 1$. And if their n_0 th ($n_0 = 0, 1, \dots, N - 3$) bits are different and other bits are the same, then

$$\begin{cases} b_{i,n}^{(1)} = b_{j,n}^{(1)}, & n = 0, 1, \dots, n_0 - 1 \\ b_{i,n}^{(1)} = \bar{b}_{j,n}^{(1)}, & n = n_0, n_0 + 1, \dots, N - 3 \end{cases} \quad (10)$$

Thus, their $(N - 2)$ th bits are also different, which is in conflict with $D^2(\gamma_i^{(1)}, \gamma_j^{(1)}, 0) = 1$. Therefore, $D^2(\gamma_i^{(1)}, \gamma_j^{(1)}, 0) \geq 2$ comes into existence. Additionally, it can be derived in the same way that the conclusion also applies to \mathcal{C}_2 .

For $\Delta m \neq 0$, we assume that in the following case, $D^2(\gamma_i^{(1)}, \gamma_j^{(1)}, 0) = 1$.

$$\begin{array}{ccccccc} i : & \gamma_{i,0}^{(1)} & \cdots & \gamma_{i,\Delta m}^{(1)} & \cdots & \gamma_{i,N-2}^{(1)} & 1 & \cdots & 0 \\ j : & 0 & \cdots & \gamma_{j,0}^{(1)} & \cdots & \gamma_{j,N-\Delta m-2}^{(1)} & \gamma_{j,N-\Delta m-1}^{(1)} & \cdots & 1 \end{array}$$

Then,

$$\begin{cases} \gamma_{i,n}^{(1)} = 0, & n = 1, 2, \dots, \Delta m - 1 \\ \gamma_{i,n}^{(1)} = \gamma_{j,n-\Delta m}^{(1)}, & n = \Delta m, \Delta m + 1, \dots, N - 2 \\ \gamma_{j,N-\Delta m-1}^{(1)} = 1 \\ \gamma_{j,n}^{(1)} = 0, & n = N - \Delta m, \dots, N - 2 \end{cases} \quad (11)$$

Thus, the case could be rewritten as

$$\begin{aligned} \gamma_i^{(1)} &= [\mathbf{0}_{1 \times \Delta m} \alpha_{\ell \times 1}^T \mathbf{0}_{1 \times (N-\Delta m-\ell-1)} \mathbf{1}]^T \\ \gamma_j^{(1)} &= [\alpha_{\ell \times 1}^T \mathbf{1} \mathbf{0}_{1 \times (N-\ell-2)} \mathbf{1}]^T \end{aligned}$$

We map $\gamma_i^{(1)}$ and $\gamma_j^{(1)}$ back to natural binary sequence according to the gray code mapping criterion. In this way, the penultimate bits of two codes are respectively $\alpha_0 \oplus \alpha_1 \oplus \cdots \oplus \alpha_{\ell-1}$ and its not value $\overline{\alpha_0 \oplus \alpha_1 \oplus \cdots \oplus \alpha_{\ell-1}}$. Therefore, $D(\gamma_i^{(1)}, \gamma_j^{(1)}, 0) \geq 2$ is workable. Additionally, this result is also suitable for \mathcal{C}_2 . ■

REFERENCES

- [1] F. Delgado-Rajo, A. Melian-Segura, V. Guerra, R. Perez-Jimenez, and D. Sanchez-Rodriguez, "Hybrid RF/VLC network architecture for the internet of things," *Sensors*, vol. 20, no. 2, pp. 478–497, 2020.
- [2] M. Durgun and L. Gokrem, "VLC4WoT: Visible light communication for web of things," *KSIIT Trans. Internet Inf. Syst.*, vol. 14, no. 4, pp. 1502–1519, 2020.
- [3] H. Yang, A. Alphones, W.-D. Zhong, C. Chen, and X. Xie, "Learning-based energy-efficient resource management by heterogeneous RF/VLC for ultra-reliable low-latency industrial IoT networks," *IEEE Trans. Ind. Informat.*, vol. 16, no. 8, pp. 5565–5576, Aug. 2019.
- [4] M. Jani, P. Garg, and A. Gupta, "On the performance of a cooperative PLC-VLC indoor broadcasting system consisting of mobile user nodes for IoT networks," *IEEE Trans. Broadcast.*, vol. 67, no. 1, pp. 289–298, Mar. 2021.
- [5] J. Vučić, C. Kottke, S. Nerretter, K.-D. Langer, and J. W. Walewski, "513 Mbit/s visible light communications link based on DMT-modulation of a white LED," *J. Lightw. Technol.*, vol. 28, no. 24, pp. 3512–3518, 2010.
- [6] P. A. Haigh and I. Darwazeh, "Real time implementation of CAP modulation with 'better-than-nyquist' pulse shaping in visible light communications," *IEEE Commun. Lett.*, vol. 24, no. 4, pp. 840–843, Apr. 2020.
- [7] R. X. Ferreira *et al.*, "High bandwidth GaN-based micro-LEDs for multi-Gb/s visible light communications," *IEEE Photon. Technol. Lett.*, vol. 28, no. 19, pp. 2023–2026, Oct. 2016.
- [8] Y.-Y. Zhang and J.-K. Zhang, "Fundamental applicability of spatial modulation: High-SNR limitation and low-SNR advantage," *IEEE J. Sel. Areas Commun.*, vol. 37, no. 9, pp. 2165–2178, Sep. 2019.
- [9] F. Zezulka, P. Marcon, Z. Bradac, J. Arm, T. Benesl, and I. Vesely, "Communication systems for industry 4.0 and the IIoT," *IFAC-PapersOnLine*, vol. 51, no. 6, pp. 150–155, 2018.
- [10] S. Rajagopal, R. D. Roberts, and S.-K. Lim, "IEEE 802.15. 7 visible light communication: Modulation schemes and dimming support," *IEEE Commun. Mag.*, vol. 50, no. 3, pp. 72–82, Mar. 2012.
- [11] K. Xu, H.-Y. Yu, Y.-J. Zhu, and H.-B. Cai, "Channel-adaptive space-collaborative constellation design for MIMO VLC with fast maximum likelihood detection," *IEEE Access*, vol. 5, pp. 842–852, 2017.
- [12] J. B. Wang, J. Yuan, X. Y. Dang, C. Ming, X. X. Xie, and L. L. Cao, "Training sequence based channel estimation for indoor visible light communication system," *Optoelectron. Lett.*, vol. 7, no. 3, pp. 213–216, 2011.
- [13] T. Fujita, D. Uchida, Y. Fujino, O. Kagami, and K. Watanabe, "A short-burst synchronization method for narrowband wireless communication systems," in *Proc. 2nd Int. Symp. Wireless Pervasive Comput.*, 2007, pp. 617–621.
- [14] H. Q. Le, H. Al-Shatri, and A. Klein, "Efficient resource allocation in mobile-edge computation offloading: Completion time minimization," in *Proc. IEEE Int. Symp. Inf. Theory*, 2017, pp. 2513–2517.
- [15] J. Beysens, Q. Wang, and S. Pollin, "Increasing throughput of dense-transmitter VLC networks through adaptive distributed MISO," in *Proc. IEEE Int. Conf. Commun.*, 2018, pp. 1–6.
- [16] C. Chen, D. A. Basnayaka, and H. Haas, "Downlink performance of optical attocell networks," *J. Lightw. Technol.*, vol. 34, no. 1, pp. 137–156, 2015.
- [17] T. Muoi, "Receiver design for digital fiber optic transmission systems using manchester (biphase) coding," *IEEE Trans. Commun.*, vol. 31, no. 5, pp. 608–619, May 1983.
- [18] O. I. Younus, H. Le Minh, P. T. Dat, N. Yamamoto, A. T. Pham, and Z. Ghassemlooy, "Dynamic physical-layer secured link in a mobile MIMO VLC system," *IEEE Photon. J.*, vol. 12, no. 3, Jun. 2020, Art. no. 7902814.
- [19] H. Chen and Z. Xu, "OLED panel radiation pattern and its impact on VLC channel characteristics," *IEEE Photon. J.*, vol. 10, no. 2, Apr. 2017, Art. no. 7901410.
- [20] Y. S. Eroğlu, Y. Yapıcı, and I. Güvenç, "Impact of random receiver orientation on visible light communications channel," *IEEE Trans. Commun.*, vol. 67, no. 2, pp. 1313–1325, Feb. 2018.
- [21] B. G. Guzman, A. L. Serrano, and V. P. G. Jimenez, "Cooperative optical wireless transmission for improving performance in indoor scenarios for visible light communications," *IEEE Trans. Consum. Electron.*, vol. 61, no. 4, pp. 393–401, Nov. 2015.
- [22] Y. Jiang, Y. Wang, P. Cao, M. Safari, J. Thompson, and H. Haas, "Robust and low-complexity timing synchronization for DCO-OFDM LiFi systems," *IEEE J. Sel. Areas Commun.*, vol. 36, no. 1, pp. 53–65, Jan. 2018.
- [23] R. Singh, T. O'Farrell, and J. P. David, "An enhanced color shift keying modulation scheme for high-speed wireless visible light communications," *J. Lightw. Technol.*, vol. 32, no. 14, pp. 2582–2592, 2014.
- [24] I. Dokmanic, R. Parhizkar, J. Ranieri, and M. Vetterli, "Euclidean distance matrices: Essential theory, algorithms, and applications," *IEEE Signal Process. Mag.*, vol. 32, no. 6, pp. 12–30, Nov., 2015.
- [25] A. Ahmad and F. Bait-Shiginah, "A nonconventional approach to generating efficient binary gray code sequences," *IEEE Potentials*, vol. 31, no. 3, pp. 16–19, May/June 2012.
- [26] C.-R. Sheu and C.-C. Huang, "A differential sliding correlation scheme for symbol timing detection in time domain synchronous OFDM systems," in *Proc. IEEE 69th Veh. Technol. Conf.*, 2009, pp. 1–5.
- [27] J.-C. Lin, "Noncoherent sequential PN code acquisition using sliding correlation for chip-asynchronous direct-sequence spread-spectrum communications," *IEEE Trans. Commun.*, vol. 50, no. 4, pp. 664–676, Apr. 2002.
- [28] H.-C. Chang, C. B. Shung, and C.-Y. Lee, "A Reed-Solomon product-code (RS-PC) decoder chip for DVD applications," *IEEE J. Solid-State Circuits*, vol. 36, no. 2, pp. 229–238, Feb. 2001.